ELSEVIER

Thermochimica Acta 289 (1996) 351–366

thermochimica acta

A method to determine heat-transfer coefficients in a heat-flow reaction calorimeter

Enio Kumpinsky

R & D Department, Ashland Chemical Company, Po Box 2219, Columbus, OH 43216, USA

Received 4 December 1995; accepted 6 March 1996

Abstract

A method to determine the overall heat-transfer coefficient in a heat-flow reaction calorimeter is presented. It can be used in situations in which calibration may not yield accurate results. For example, it does not require any holding period at or near the temperature of interest, which may interfere with the chemical process. Also it can provide a realistic temperature difference between the reactor and the jacket when dealing with viscous liquids. The proposed technique is based on the solution of the RC1 energy balance and only calorimeter data and parameters are utilized in the calculations.

Standard calibration may still be necessary in conjunction with temperature ramps to evaluate specific heats. However, this procedure can be carried out at a lower temperature, away from the reaction conditions. An important concept presented in this work is the dimensionless group we shall call the *heat-loss number*. With it we can determine the overall heat-transfer coefficient with increased accuracy and have a realisitc account of heat losses.

Keywords: Calibration; Coefficient; Heat loss; Heat-transfer; Overall

NOMENCLATURE

A	wetted area for heat transfer between the reactor and the jacket/m^2
$A3$	measured value representing the difference between the exit and the inlet temperatures of the reflux condenser cooling fluid/°C
Bn	mass in the reactor from balance n/kg
C_i	heat capacity of all internal fittings/J kg^{-1}
C_{pc}	specific heat of the cooling fluid through the reflux condenser/J $kg^{-1}K^{-1}$

0040-6031/96/$15.00 © 1996 – Elsevier Science B.V. All rights reserved
PII S0040-6031(96)03007-9

C_{p0}	specific heat of the initial mass in the reactor/J $kg^{-1}K^{-1}$
C_{pBn}	specific heat of dosing stream from balance n/J $kg^{-1}K^{-1}$
m_c	mass of cooling fluid in the reflux condenser/kg
m_{r0}	initial mass in the reactor/kg
N	number of dosing streams, dimensionless
N_α	heat-loss number, defined by Eq. (7), dimensionless
P_v	vapor pressure/MPa
Q_a	heat accumulation by the reaction mass/W
Q_c	calibration power/W
Q_{cond}	heat flow through the reflux condenser/W
Q_{dos}	heat input due to dispensing/W
Q_f	heat flow through the reactor walls/W
Q_i	heat accumulation by the internal fittings/W
Q_{loss}	heat losses through the reactor head assembly by radiation and conduction/W
Q_r	heat generation rate of chemical or physical reaction/W
Q_{stir}	energy input due to stirrer/W
T_a	adjusted jacket temperature/°C
T_{amb}	ambient temperature next to the reactor/°C
T_{BN}	temperature of the dosing stream n/°C
T_r	reactor temperature/°C
U	overall heat-transfer coefficient of the reactor wall/W $m^{-2}K^{-1}$
V_v	virtual volume, i.e., the apparent volume of the liquid in the reactor due to the formation of a vortex/l
α	heat-loss coefficient/W K^{-1}

1. Introduction

The overall heat-transfer coefficient of the reactor wall is a key parameter for the thermal evaluation of experiments in a heat-flow reaction calorimeter. It is needed to obtain specific heats and to perform energy balances. The concepts of a typical heat-flow reaction calorimeter have been described elsewhere [1–3] and they well be omitted here. The standard procedure to determine U is calibration. This is done with an immersion heater that releases a known amount of thermal energy for a fixed period of time. After the experiment, this information can then be processed to yield the overall heat-transfer coefficient.

Standard calibration is the preferred method to determine the overall heat-transfer coefficients, but there are situations in which it should be avoided. It takes a minimum of about 45 min to complete a calibration, baselines included. If a mixture cannot be held at a certain temperature for this period of time and becomes unstable, the calibration will be incorrect. In addition, when dealing with viscous liquids during a nonisothermal process, the difference between the reactor and jacket temperatures may be quite different from the one realized with calibration.

It is desirable to develop a technique that complements calibration, to be used in situations where the latter may lack in accuracy. We shall call this technique the *dynamic method*, because an active event is needed to make it work, such as a temperature ramp or dosing. Calibration and ramp can be used to yield the specific heat of the reaction mass, but this can be done at a lower temperature where interference with the chemical process does not occur. Specific heat usually varies less with temperature than does the overall heat-transfer coefficient. If calibration is not feasible even at lower temperatures, an alternative is to use a thermodynamic software package to calculate C_p, if the molecular species are simple enough. A temperature ramp not only leads the charge to the reaction temperature but also provides data to calculate U by the dynamic method. The overall heat-transfer coefficient can be measured as close as possible to the hold temperature, until the reaction becomes thermally detectable. The isothermal or nonisothermal dosing of a raw material can also be handled by the dynamic method.

A procedure was developed to determine the overall heat-transfer coefficient in vessels with one jacket or one coil [4]. Later [5], the concept was extended to include vessels with any combination of jackets and coils. The idea of thermal consistency was discussed, showing that macroscopic balances are more robust than those obtained from the integration of differential equations. Indeed, the latter depend only on the initial and final vessel temperatures, thus failing to account for intermediate values. Direct application of differential equations may not be practical with thermal data from the large-scale equipment of many manufacturing facilities. This is because the interval of data collection might be broad, making it impossible to calculate accurately the instantaneous changes in vessel temperature . With either microscopic or macroscopic balances, the equations must be solved with computer programming.

Laboratory heat-flow reaction calorimeters have the ability to collect data at very short time intervals, say, every two to ten seconds. As a consequence, they can accurately determine the instantaneous rates of change of the reactor temperature. With this capability, the use of programming languages becomes unnecessary. They have software that can evaluate U without any external treatment. However, temperature data can be imported into a spreadsheet and used to calculate the overall heat-transfer coefficient by the dynamic method, which is an extension of the techniques from Refs. [4] and [5]. If so desired, this U can then be applied to the evaluation program of the calorimeter or to a spreadsheet to calculate heat flows.

As described so far, the dynamic method presents the same shortcomings of the standard calibration regarding interference from thermal losses when a heated cover is not available. These losses may be significant at higher temperatures and for the sake of accuracy they must be accounted for. The calorimetric evaluation program usually has a mechanism to include a heat-loss term in the energy balance. The difficulty with this approach is that this term requires the knowledge of a constant coefficient that cannot be calculated by the standard program. A default may be provided to the user, but its value might not be realistic for the conditions of a particular experiment. Furthermore, the heat-loss coefficient varies with temperature. A method is proposed in Section 4 to calculate the heat-loss coefficient and to increase the accuracy of the energy calculations, whether standard calibration or the dynamic method is used to calculate U.

2. Energy balance

A general energy balance for a heat-flow reaction calorimeter can be written as

$$\begin{pmatrix}\text{Heat}\\ \text{Accumulation}\end{pmatrix}=\begin{pmatrix}\text{Heat}\\ \text{Inflow}\end{pmatrix}-\begin{pmatrix}\text{Heat}\\ \text{Outflow}\end{pmatrix} \tag{1}$$

Expanding Eq. (1)

$$(Q_a + Q_i) = (Q_r + Q_c + Q_{stir}) - (Q_f + Q_{dos} + Q_{loss} + Q_{cond}) \tag{2}$$

The symbols can be found in the Nomenclature. The Q_{stir} term can be neglected, unless the viscous effects are extreme. Expanding Eq. (2) we obtain the general energy balance equation for a heat-flow reaction calorimeter

$$\begin{aligned}\left[m_{r0}C_{p0} + \sum_{n=1}^{N} Bn(t)C_{pBn} + C_i(t)\right]\frac{dT_r}{dt} &= Q_r(t) + Q_c(t) + Q_{stir}(t)\\ &\quad - U(t)A(t)[T_r(t) - T_a(t)]\\ &\quad - \sum_{n=1}^{N} C_{pBn}\frac{dBn}{dt}(t)[T_r(t) - T_{Bn}(t)]\\ &\quad - \alpha[T_r(t) - T_{amb}(t)] - \frac{dm_c}{dt}C_{pc}A3(t)\end{aligned} \tag{3}$$

The heat-transfer area A is based on the wetted surface, i.e., the portion of the reactor walls in contact with the liquid. The user visually determines the volume that corresponds to the wetted area and enters the information in the computer interface, at the beginning and during an experiment. Corrections can always be made at the time of data evaluation. This parameter is usually known as the virtual volume.

3. Experimental apparatus

The instrument used in this work was the RC1 Reaction Calorimeter, manufactured by Mettler Toledo, equipped with the AP01 glass atmospheric pressure reactor [6]. Refs. [1], [2], and [3] provide an excellent review on the operation and applications of this calorimeter. For the AP01 reactor, we can assume that

$$A = 0.0070 + 0.0348V_V \tag{4}$$

This is valid for a reasonable volume of liquid inside the reactor, since the correlation is false for $V_V = 0$. The anchor agitator and the temperature sensor were made of Hastelloy C-276, and the glass calibration probe released 23.2 W, on average, when turned on. The data were collected every six seconds.

4. Examples and discussion

The usefulness of the techniques of this work is better assessed by means of examples. Example 1 covers the heating and cooling of water. Example 2 embodies the dosing of

water into a solution of carboxymethyl cellulose, sodium salt, while the reactor temperature is ramped. Example 3 shows the application of the dynamic method with an industrial product that undergoes a chemical reaction. Example 4 introduces the heat-loss number, a dimensionless group used to calculate heat losses in the calorimeter. Example 5 deals with the effect of heat losses on heat-flow calculations. Example 6 illustrate the use of the heat-loss number with calibration to improve the accuracy of heat-flow calculations.

4.1. Example 1

Deionized water was charged to the calorimeter to compare the calibration and dynamic methods for a low viscosity liquid. The data are: $m_{r0} = 1.20$ kg, $C_{p0} = 4184$ J kg^{-1} K^{-1}, $C_i = 130$ J K^{-1}, $\alpha = 0.1$ W K^{-1} (RC1 default), and $V_v = 1.30\,\ell$, which yields $A = 0.0522$ m^2 from Eq. (4). The agitator rotational speed was 100 rpm. Calibrations were performed every 5°C, from 25 to 45°C. Heating and cooling ramps were developed from 20 to 50°C and vice-versa, so that the temperature profiles were well developed and stable in the 25 to 45°C range. The application of Eq. (3) to this example yields

$$U(t) = \frac{(m_{r0}C_{p0} + C_i)\dfrac{dT_r}{dT} + \alpha[T_r(t) - T_{amb}(t)]}{A[T_a(t) - T_r(t)]} \tag{5}$$

Note that the RC1 uses a constant value for the ambient temperature, but the dynamic method allows for T_{amb} dependence with time. Different rates were used for cooling and heating, and the curves are summarized in Fig. 1. From A to B the cooling rate was -1°C min^{-1}, from B to C the heating rate was +1°C min^{-1}. From C to D the

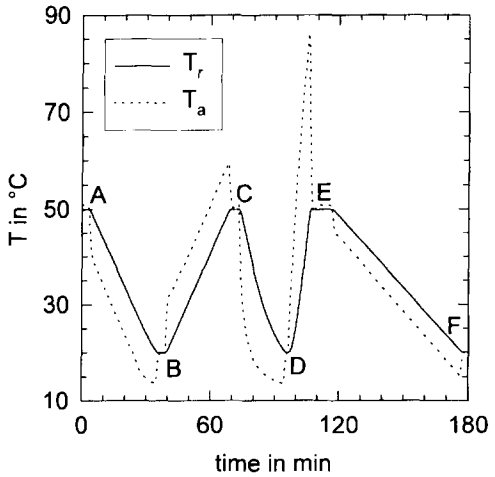

Fig. 1. Heating and cooling temperature ramps of Example 1.

T_r setpoint was changed from 50 to 20°C, so that the cooling occurred as quickly as possible. At D the setpoint was switched back to 50°C, and T_r rapidly reached the goal temperature at E. Finally, T_r was ramped from 50 to 20°C at -0.5°C min^{-1}, E to F.

Fig. 2 displays the outcome of Example 1. It shows the results of dynamic method calculations with Eq. (5) and calibration. In order to reduce some noise of the plotted data, each point represents the average of 21 points in the adjacent ± 1 min. For cooling there is a very good agreement between the two methods, because the T_r-T_a values were also similar. A small deviation occured for the -0.5°C min^{-1} case (E–F) at 45°C because heat losses began to take effect. Such losses are more prominent with slow cooling, inducing a reduction in T_r-T_a, and, as a consequence, an increase in Uas per Eq. (5). For heating the situation is reversed. With slow heating (B–C), the deviation of U from the calibration values is relatively small while for a quick heat-up (D–E), it yields significantly higher U values. In this case the wall effects were conspicuous even with a low viscosity fluid. This finding suggests that U calculated by calibration should be used very cautiously with highly endothermic processes, even if the viscosity is low. Calibration may underestimate the heating needs of such processes by yielding lower than real U values.

Comparing one-point with averaged data, the difference between the two sets was negligible. However, averaging reduced the experimental noise, which was small to begin with. Computations were also done using Eq. (5) in integral form, with term-by-term integration. Trapezoidal rule and higher order Newton–Cotes formulae were used in the ± 1 min interval. Again, there were no noticeable differences from the one-point calculations, except for noise reduction, since integration is an averaging method. The choice of a small temperature interval for U evaluation may be critical when the physical properties of the reactor fluid change, especially the specific heat.

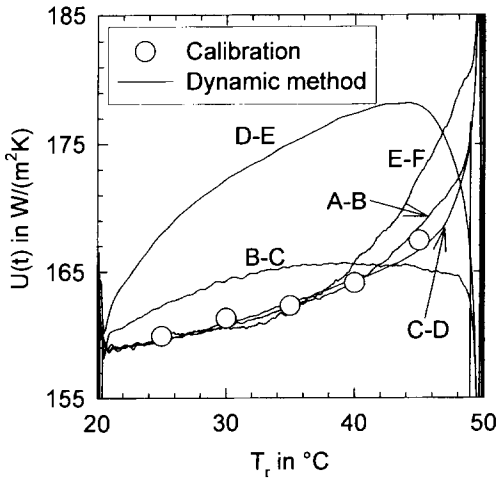

Fig. 2. Effect of the reactor temperature on the overall heat-transfer coefficient of Example 1.

4.2. Example 2

A total of 0.89kg of a 1.0% solution of carboxymethyl cellulose, sodium salt, with viscosity of 3000 cP at 25°C, was added to the calorimeter. The temperature T_r was set to 65°C with the agitator at 110 rpm. Then, 0.5 kg of water was dosed into the calorimeter at a rate of 10 g min^{-1} for 50 min, as a temperature ramp from 65 to 45°C was in effect for the duration of the feed. The product was a liquid with viscosity of 1000 cP at 25°C. Calibrations and temperature ramps were executed before and after the feed to determine the overall heat-transfer coefficient and specific heat by the standard RC1 methods. For this test, we have: $m_{r0} = 0.89$kg, $C_{p0} = 3870\ J\,kg^{-1}\,K^{-1}$, $C_i = 130\ J\,K^{-1}$, $\alpha = 0.1\ W\,K^{-1}$ and $V_v = 0.97\ell$ at the beginning and $1.47\ \ell$ at the end (real measurements). From Eq. (3) we obtain the energy balance for this example.

$$U(t) = \frac{[m_{r0}C_{p0} + B1(t)C_{pB1} + C_i]\dfrac{dT_r}{dt} + C_{pB1}\dfrac{dB1}{dt}(t)[T_r(t) - T_{B1}(t)] + \alpha[T_r(t) - T_{amb}(t)]}{A[T_a(t) - T_r(t)]} \tag{6}$$

Fig. 3 displays the results of the experiments. The dotted line shows the linear variation of U along the experiment by means of calibration before and after the dosing. The solid line is the result of dynamic calculations, using Eq. (6) and averaging the results over $\pm$ 1 min for each point to decrease some of the noise. The dashed line represents the linear regression of the solid curve for $B1(t)$ between 0.05 and 0.45 kg, to avoid the end effects. The agreement between the regressed data of the dynamic method and calibration is very good, showing that calibration, an exothermic process, can be used for endothermic processes as long as the temperature differences are not too great.

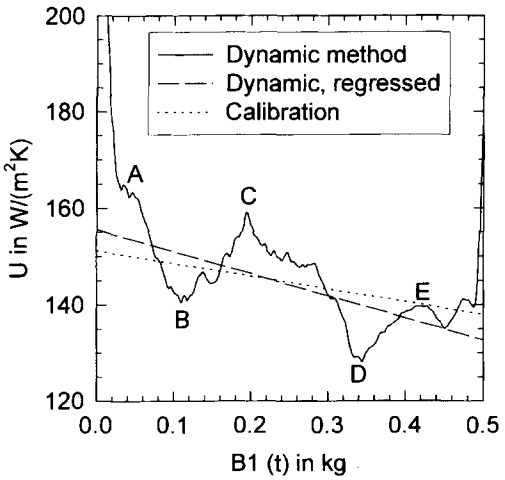

Fig. 3. Overall heat-transfer coefficient as a function of dispensed water mass for Example 2.

Typical values of $T_a(t) - T_r(t)$ during the water feed were about 5°C. The shape of the solid line in Fig. 3 reflects the complex nature of this experiment. From A to B, as the reactor temperature drops, so does the heat-transfer coefficient. From B to C, the decrease in viscosity with water addition becomes the dominant effect and U increases. From C to D, the decrease in temperature is the controlling mechanism and U goes down. From D to E, the lowering in viscosity again becomes the prevailing effect, resulting in an increase in the heat-transfer coefficient.

4.3. Example 3

A resol is a phenol–formaldehyde resin whose reaction is catalyzed by a base, such as an amine or a hydroxide of an alkali metal. Before adding the catalyst, a ramp from 25 to 30°C was used to calculate the specific heat, and standard calibration at 30°C determined the overall heat-transfer coefficient at that temperature. The question is: Can we obtain a more accurate value of U at the reaction temperature of 65.5°C? This system shows thermally detectable reactivity beginning at about 55°C even without catalyst, so calibration at or near 65.5°C is not an option. Standard calibration just below 50°C is not viable either because the mixture of this particular experiment was not chemically stable for the time required to conduct calibration. The data for this example are $m_{r0} = 1.20\,\text{kg}$, $C_{p0} = 2806\ \text{J kg}^{-1}\text{K}^{-1}$ obtianed by the above procedure, $C_i = 130\ \text{J K}^{-1}$, $\alpha = 0.1\ \text{W K}^{-1}$, $T_{amb} = 23°\text{C}$, and $V_v = 1.23\,\ell$, from which $A = 0.0499\ \text{m}^2$ using Eq. (4).

Fig. 4 shows the profiles for the heating ramp beginning at 45°C, at which point the base was added. The dynamic method is versatile enough to be used in an interval in which dT_r/dt is not yet stable. However, we must be beyond the initial kick, which occurs between 1 and 2 min in Fig. 4. The two vertical lines bound the range of T_r that

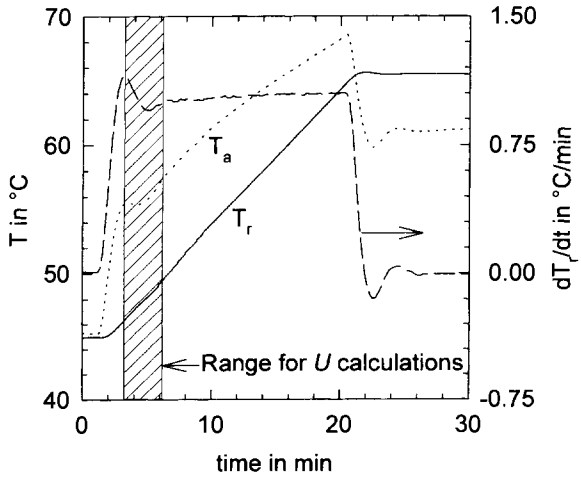

Fig. 4. Temperature ramps and heating rate to evaluate the overall heat-transfer coefficient of Example 3 by the dynamic method.

we used with Eq. (5) to calculate the overall heat-transfer coefficient with the dynamic method. The range is narrow indeed. On the one hand, the temperature has to be somewhat higher than 45°C, so that a reasonably stable ramp is established. On the other hand, it cannot exceed 50°C, towards which the reaction becomes significant. In spite of the fact that the heating ramp is not fully established in the 46.2–49.4°C range, all values of U were restricted to the narrow 159.8–162.5 $W m^{-2} K^{-1}$ band, with an average of 160.8 $W m^{-2} K^{-1}$ and standard deviation of 0.74 $W m^{-2} K^{-1}$. The calibration at 30°C yielded at U value of 156 $W m^{-2} K^{-1}$, so at 65.6°C one would expect an overall heat-transfer coefficient of about 165–170 $W m^{-2} K^{-1}$. The low end, 165 $W m^{-2} K^{-1}$ is more likely to be correct, since the calculation above is based on a negative T_r-T_a. This difference is positive during the exotherm, in which case some wall effects ought to be considered.

This is an instance where the combination of calibration and dynamic method affords the best out of the heat-flow calorimeter. Calibration is utilized in the calculation of C_{p0} and provides a reference for U at a lower temperature. The dynamic method, using this specific heat and the RC1 temperature data, is used to calculate U at the maximum temperature prior to the onset of the chemical reaction. Good sense then dictates how to extrapolate U to the reaction temperature.

4.4. Example 4

We will now discuss a technique that accounts for heat losses in the calorimeter. Using a simulator, Leach [7] determined heat-loss factors as a function of temperature for three different liquids, one of which was water. It is our intent to present a method that is self-contained, using exclusively RC1 data that can be processed in a spreadsheet.

T_r and T_a should be identical at room temperature. If there is a small discrepancy, this can be added or subtracted from the T_r-T_a values of the experiments. An alternative is to activate the Maintenance Program to set this difference to zero. Once this preliminary procedure is complete, the reactor temperature is stablized at different setpoints. Obviously, we should expect higher heat losses with increasing temperatures. The energy balance is simple for this steady-state situation. From Eq. (2) we obtain $Q_f + Q_{loss} = 0$. Using the pertinent terms from Eq. (3) we get

$$N_\alpha = \frac{\alpha}{UA} = \frac{T_a - T_r}{T_r - T_{amb}} \tag{7}$$

where the dimensionless group N_α is the heat-loss number. N_α is the ratio of the heat-loss coefficient to the product of the overall heat-transfer coefficient and the heat-transfer surface area. It is a measure of the magnitude of heat losses with respect to the heat transferred from the reactor to the jacket. Its numerical value depends on the operating conditions of the vessel, so it is a property of the fluid and the calorimeter, and not of the instrument alone.

With 1.200 kg of water in the reactor, anchor agitator at 100 rpm, T_{amb} = 23°C, A = 0.0522 m^2, C_{p0} = 4184 $J kg^{-1} K^{-1}$, and C_i = 130 $J K^{-1}$, we set T_r from 40 to

80°C, stabilizing the temperature at every 10°C. At each of these temperatures we obtained the steady-state T_a-T_r. Heat losses are due to radiation and convection in the vapor space. As the reactor temperature is raised toward the boiling point, vaporization at the liquid surface and condensation of the vapor on the inner side of the cover becomes the dominant mechanism for heat loss. The reactor cover was insulated with white fiber glass to minimize heat losses by radiation. If a heated cover is used, condensation is avoided and heat losses can be minimized or neglected. The results of this experiment are summarized in Fig. 5.

Vapor pressures of liquids are known to fit the Antoine equation [8], at least in a certain temperature range. N_α is very well represented by a correlation with the Antoine structure (solid line) as Fig. 5 indicates, which is valid between 40 and 80°C. P_v and N_α move almost parallel to each other, a clear indication that vaporization is responsible for most of the heat losses in this example. The Anotine equation is usually written in kelvins, but degrees celsius is acceptable because the denominator of the exponent is given as the difference between T_r and a constant. Our exponential coefficients, -157.7 and -10.9, are smaller than those of water reported in the literature [8], i.e., -3816.4 and 227.0 (converted to degrees celcius). Calculations indicate that the Antoine exponential coefficients for water yield good estimates, but our coefficients provide slightly better results.

4.5. *Example 5*

We will now expand the technique described in Example 4 to determine U and α, and to calculate heat flow using the dynamic method. The system of the previous example was heated to 80°C and stabilized over 30 min. The calibration heater was then turned on to determine U. After a 20-min stabilization, the reactor temperature was ramped

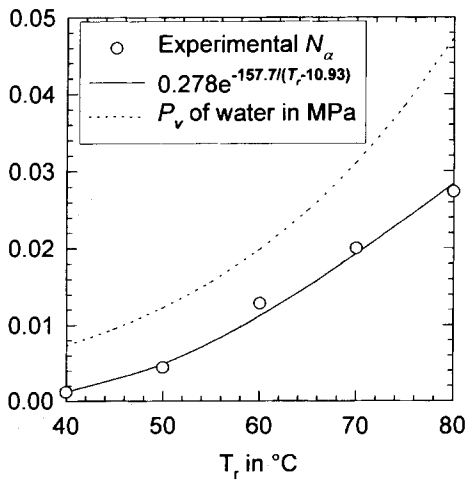

Fig. 5. Effect of the reactor temperature on water vapor and the heat-loss number of Example 4.

from 80 to 20°C at a rate of -0.5°C min^{-1}. After a 20-min hold, the calibration heater was activated to determine U. Twenty minutes thereafter the experiment was terminated. With the calibration data, we determined UA as 9.9 and 8.3 W K^{-1} at 80 and 20°C, respectively. This compares well with the experiments of Leach [7], whose interpolated data yielded 9.8 and 8.6 W K^{-1} at 80 and 20°C. The calibrations are used to compare the dynamic method with the standard thermal evaluation. With known N_α, we can write, based on Eq. (7).

$$\alpha = UAN_\alpha \tag{8}$$

Eqs. (5) and (8) form a set of two equations and two unknowns, U and α. Introducing Eq. (8) into Eq. (5) and isolating U we get

$$U(t) = \frac{(m_{r0}C_{p0} + C_i)\dfrac{dT_r}{dt}}{A\{T_a(t) - T_r(t) - N_\alpha[T_r(t) - T_{amb}(t)]\}} \tag{9}$$

The solid line in Fig. 6 represents the calculated U values as a function of T_r. The shape of this curve is quite different from the dotted line, which depicts the linearized calibration profile of U between 80 and 20°C. Due to significant heat losses, T_r-T_a was underestimated during calibration, thus leading to higher than real overall heat-transfer coefficients. The method of this work accounts for these heat losses by adding the term containing N_α in the denominator of Eq. (9). We observe that U remains in the 164–169 W m^{-2} K^{-1} range between 80 and 50°C. The discrepancy with calibration U values at higher temperatures may be due to the fact that there is no equilibrium with the dynamic method. The system is in constant change, including the temperature profile in the glass wall, in the overhead and in contact with the liquid. As the water is

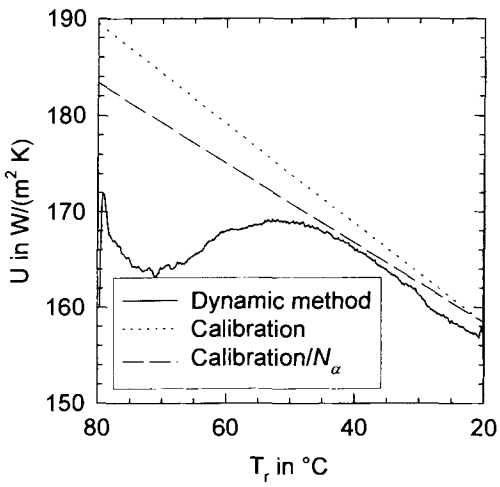

Fig. 6. Overall heat-transfer coefficient as a function of the reactor temperature of Examples 5 and 6.

cooled below 50°C, the dynamic overall heat-transfer coefficient declines in an essentially linear fashion with the temperature.

With known U, we can go back to Eq. (8) and calculate the heat-loss coefficeint α. The results are summarized in Fig.7. Like N_α, the heat-loss coefficient α can be correlated to the Antoine equation [8], and the two exponential coefficients are the same as those of N_α (Fig. 5). Fig. 7 shows that the R C1 default for α, 0.1 W K^{-1}, is reasonable only in the vicinity of 60°C for this particular example. The results of Fig. 7 are valid for the system of Examples 4 and 5 only, and should not be used under any other conditions. It is advisable to carry out the experiments with the raw materials and parameters of a particular reactor and formulation, since α depends on the vapor pressure of the liquid.

Now we can compare the cumulative heat obtained by two modes, i.e., dynamic method using Eq. (9) with α correction, and R C 1 Evaluation Program with the default $\alpha = 0.1$ W K^{-1}. The ordinate of Fig. (8) for the dynamic method was obtained from

$$\int_0^t [Q_f(\tau) + Q_{loss}(\tau)]d\tau = \int_0^t \{U(\tau)A[T_r(\tau) - T_a(\tau)] + \alpha(\tau)[T_r(\tau) - T_{amb}]\}d\tau$$
$$= \int_0^t U(\tau)A\{[T_r(\tau) - T_a(\tau)] + N_\alpha(\tau)[T_r(\tau) - T_{amb}]\}d\tau \quad (10)$$

and plotted against $T_r(t)$, where τ is an integration variable. In spite of the nonlinearity of $U(t)$ at higher temperatures, the dynamic method yielded the expected straight line in Fig. 8 with virtually no experimental noise. The R C 1 evaluation (dotted line) generated a profile with a slight curvature. The final result for the cumulative heat was

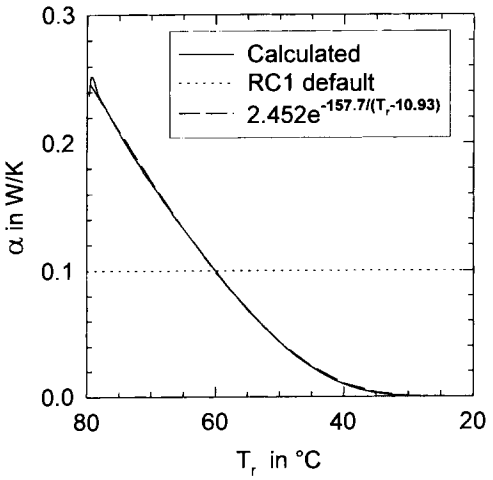

Fig. 7. Dependence of the heat-loss coefficient on the reactor temperature of Example 5, dynamic method.

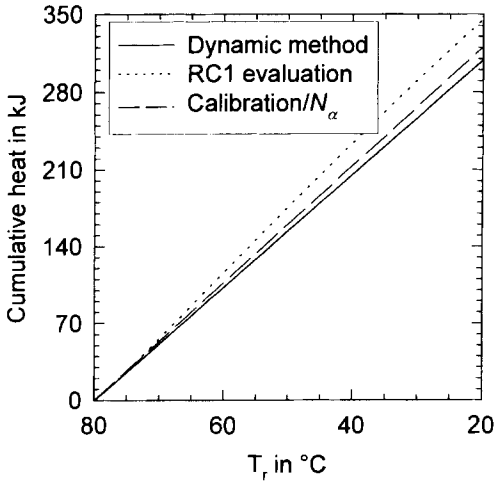

Fig. 8. Cumulative heat with the cooling ramp of Examples 5 and 6.

308.3 kJ for the dynamic method and 345.5 kJ for the R C 1 evaluation. For this simple example, we can easily verify the correct answer, by integrating the cumulative heat term

$$-\int_0^t Q_a(\tau)\mathrm{d}\tau = -\int_0^t (m_{r0}C_{p0} + C_i)\frac{\mathrm{d}T_r}{\mathrm{d}\tau}\mathrm{d}\tau = (m_{r0}C_{p0} + C_i)[T_r(0) - T_r(t)] \tag{11}$$

The substitution of numerical values into Eq. (11) yields

$$-\int_0^t Q_a(\tau)\mathrm{d}\tau = \left(1.2\,\mathrm{kg} \times 4184\frac{\mathrm{J}}{\mathrm{kg\,K}} + 130\frac{\mathrm{J}}{\mathrm{K}}\right) \times (80-20)\,\mathrm{K} \times \frac{1\,\mathrm{kJ}}{1000\,\mathrm{J}} = 309.0\,\mathrm{kJ}$$

There is an almost perfect fit between the theoretical value and the one calculated by the dynamic method. The error of the R C 1 evaluation with the default heat-loss correction was significant: $100 \times (345.5\text{-}309.0)/309.0 = 11.8\,\%$. Calibration is still the most convenient method to generate overall heat-transfer coefficients, and it is not our intent to claim advantages of the dynamic method over calibration. Instead, we can build on the knowledge of this example to improve the accuracy of calibration and heat-flow calculations.

The contributions in percent of the heat-flow and heat-loss terms for water cooling of this example can be assessed in Fig. 9. The cumulative heat-loss contribution increased steadily from 80 to about 65°C, after which it stabilized. At temperatures below 40°C the participation of the heat-loss term was negligible. This is also visualized in Fig. 10, where the instant contribution of thermal loss to the total heat flow is plotted against the reactor temperature. With a participation on the order of 30% at 80°C, the contribution of the heat-loss term decays exponentially with T_r. From Figs. 9 and 10 it is obvious that a constant value of α does not apply to this situation.

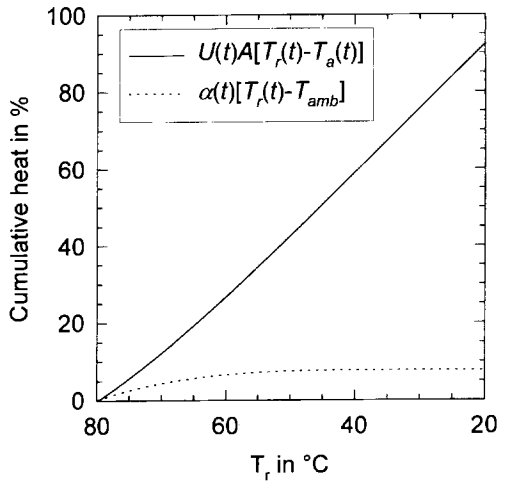

Fig. 9. Contributions of heat flow through the wall and heat losses for the water cooling of Example 5, dynamic method.

4.6. Example 6

We will now elucidate the procedure to obtain improved overall heat-transfer coefficient and heat flow, using standard calibration and correction for heat loss. From Eq. (2) we can write $Q_c = Q_f + Q_{loss}$ for the regression range during calibration. Then, using the appropriate terms of Eq. (3) in combination with Eq. (8) we get

$$U = \frac{\int_{t_{r0}}^{t_{rf}} Q_c(\tau)\,d\tau}{A\int_{t_{r0}}^{t_{rf}} \{[T_r(\tau) - T_a(\tau)] + N_\alpha[T_r(\tau) - T_{amb}]\}\,d\tau} \tag{12}$$

Where the subscripts r0 and rf refer to the beginning and end of regression time, while the calibration probe is turned on. With virtually unchanged T_r-T_a values, it is not difficult for the user to identify the regression range. Q_c, T_r, and T_r-T_a data are imported into a spreadsheet and the integrations of Eq. (12) can be done with the trapezoidal rule. For the system of Examples 4 and 5, we determined $U = 183.4\,W\,m^{-2}\,K^{-1}$ at 80°C. This is somewhat less than the value of $189.4\,W\,m^{-2}\,K^{-1}$ calculated by the Evaluation Program, which has baseline correction but does not include the heat-loss term. The U value at 20°C was not affected by heat losses. The linearization of U is displayed by a dashed line in Fig. 6. Now, with this linearized $U(t)$, we employ Eq. (10) to determine the cumulative heat that was removed from the water in the reactor. Using the default $\alpha = 0.1\,W\,K^{-1}$, the outcome at the end of the cooling ramp (20°C) was 320.5 kJ, with a deviation of $100 \times (320.5–309.0)/309.0 < 3.7\%$. This is a significant improvement over the results obtained directly from the R C 1 Evaluation Program.

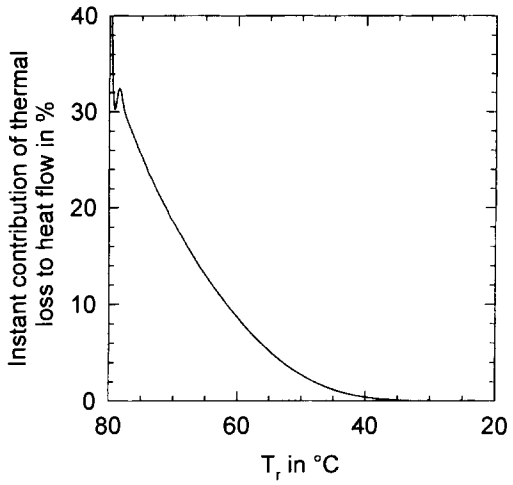

Fig. 10. Instantaneous contribution of heat losses to the heat flow of Example 5, dynamic method.

5. Conclusions

A dynamic method is presented to complement calibration in the establishment of heat-transfer parameters for the RC1 Reaction Calorimeter. In order to work, the technique requires a change in the system, such as dosing or a temperature ramp. There is a very good agreement between the dynamic method and standard calibration when the T_r-T_a values are similar and heat losses are taken into account. The procedure of this work is useful to estimate U values at the reaction conditions by extrapolating data obtained at lower temperatures. It is also recommended over calibration when dealing with highly reactive viscous materials, since $T_r - T_a$ might be significantly different from the value obtained during calibration.

This work introduced the dimensionless group N_α, i.e., the heat-loss number. The accuracy of heat-flow evaluations is greatly enhanced at higher temperatures with the use of N_α. This is true with calibration and the dynamic method. A spreadsheet is all that is needed to apply the techniques of this work. No computer programming is required.

References

[1] B. Grob, R. Riesen and K. Vogel, Reaction calorimetry for the development of chemical reactions, Thermochim. Acta, 114(1987)83–90.

[2] J.P. Jacobsen, Reaction calorimeter. A useful tool in chemical engineering, Thermochim. Acta, 160 (1990) 13–23.

[3] R.N. Landau and D.G. Blackmond, Scale-up heat transfer based on reaction calorimetry, Chem. Eng. Prog., November (1994) 43–48.

[4] E.Kumpinsky, Experimental determination of overall heat transfer coefficient in jacketed vessels, Chem. Eng. Comm., 115 (1992) 13–23.

[5] E. Kumpinsky, Heat-transfer coefficients in Agitated vessels. Sensible heat models, Ind. Eng. Chem. Res., 34 (1995) 4571–4576.
[6] Mettler Toledo RC1e Reaction Calorimeter Operating Instructions, Switzerland, November 1995, Chap. 2 and 3.
[7] J.T. Leach, Sr., Is heat loss from the AP01 vessel due to radiation, vapor pressure or both?, Proceedings, Mettler Toledo, 5th RC User Forum USA, San Antonio, Texas, October 4–7, 1992.
[8] R.C. Reid, J.M. Prausnitz and T.K. Sherwood, The Properties of Gases and Liquids, McGraw-Hill, New York, 3rd edn., 1977, p.184.